

Optimal Conditions for Alkaline Delignification Process in Cellulose Isolation from Sengon Wood Sawdust

Intan Martha Cahyani^{1,4}, Adhyatmika², Endang Lukitaningsih³, Teuku Nanda Saifullah Sulaiman^{2*}

¹Doctoral Program of Pharmaceutical Science, Faculty of Pharmacy, Universitas Gadjah Mada, Yogyakarta, 55281, Indonesia

²Department of Pharmaceutics, Faculty of Pharmacy, Universitas Gadjah Mada, Yogyakarta, 55281, Indonesia

³Department of Pharmaceutical Chemistry, Faculty of Pharmacy, Universitas Gadjah Mada, Yogyakarta, 55281, Indonesia

⁴STIFAR "Yayasan Farmasi", Letjend Sarwo Edie Wibowo KM 1, Semarang, 50192, Indonesia

*Corresponding author: tn_saifullah@ugm.ac.id

Abstract

Sengon wood sawdust (SWS) is a solid waste of the wood industry with the potential as a source of cellulose and can increase its economic value. However, cellulose in plants is tightly bound to lignin which is called lignocellulose therefore needs to be delignified before utilization. In this study, we determined the optimum conditions for delignification from sengon wood sawdust cellulose (SWSC). Optimization variables were determined with the parameter of obtained hemicellulose, cellulose, and lignin content. The optimization of SWSC delignification was then carried out using the factorial design by analyzing the effect of sodium hydroxide (NaOH) concentration (2% - 10%) and ratio (SWS : NaOH solution) (1:10 - 1:80) on hemicellulose, cellulose, and lignin content. Optimal conditions were obtained at 2% NaOH (1:19.20) with concentrations of 8.01% hemicellulose, 52.49% cellulose, and 22.2% lignin. One sample T-test analysis of predictive and research values of hemicellulose, cellulose, and lignin showed insignificant results ($P > 0.05$) which means that the optimization equation proved valid to determine the optimum conditions for cellulose delignification of sengon wood sawdust. FT-IR analysis, SEM imaging, and particle size distribution (PSA profile) showed that the cellulose produced under these conditions has similar characteristics to the standard of Avicel® PH 102.

Keywords

Characterization, Cellulose, Delignification, Optimization, Sengon Wood Sawdust

Received: 4 June 2023, Accepted: 13 August 2023

<https://doi.org/10.26554/sti.2023.8.4.666-674>

1. INTRODUCTION

Sengon is a woody plant widely cultivated on the island of Java, and it is an important raw material for wood industries (Rahmawati et al., 2019). The high market interest is due to the attractive texture, color, and fiber of sengon wood to be used as furniture material and has high potential as a source of biomass-based energy (Siregar et al., 2019). As a consequence, this will result in the abundant waste produced by the wood industry with low-to-no value. The reported utilization is mostly in the manufacture of particle boards (Laksono et al., 2022) and electrocatalysts (Sudarsono et al., 2020), while in the pharmaceutical industry, it is still minimal. Interestingly, sengon wood contains high cellulose content, namely 45,42% cellulose, 21% hemicellulose, 26,5% lignin, and 7,08% ash (Hartati et al., 2010). The use of cellulose is extensive and documented (Taher et al., 2023; Bangar et al., 2023; Wang et al., 2023). The cellulose, when provided in the appropriate quality, can be used as a pharmaceutical excipient with a higher value. The

quality needed to reach the pharmaceutical grade includes its purity, which involves the separation of cellulose in the wood sawdust from the other components.

Cellulose is a glucose polymer with a strong molecular structure and high molecular weight. It has the molecular formula of $2(C_6H_{10}O_5)_n$ where n is the degree of 1500 polymerization and 243,000 of the molecular weight (Sheskey et al., 2017). The longer a cellulose chain, the stronger the fiber. The source and the extraction process will affect the variation in the degree of polymerization. Natural cellulose is almost always bound to other materials, such as lignin and hemicellulose; while in plants, cellulose is strongly bound to lignin which is called lignocellulose. The lignocellulose needs to be delignified to break the bond and obtain the free cellulose. In the last decade, delignification has become the focal point of agro-industrial waste processing (Mukherjee et al., 2018).

Apart from releasing bonds in lignocellulosic, delignification also affects the effectiveness of the cellulose hydrolysis process by increasing surface area and cell wall porosity and

maximizes cellulose conversion (Kundu et al., 2021). It can be carried out by using acids like sulfuric, hydrochloric, phosphoric, oxalic, and maleic acids, bases like ammonium, potassium, calcium, and sodium hydroxide (Sanchez, 2007), and organic solvents like ethanol (Cheng et al., 2018). Among those three methods, the alkaline method is the most widely used for delignification for its effectiveness. Alkaline solutions such as NaOH can modify lignin by cutting the xylan and lignin bonds (Trache et al., 2016; Ameram et al., 2019).

Several delignification studies using NaOH solution with various concentrations have been carried out including on wheat straw at 2% (Krivokapić et al., 2020), *Saccharum spontaneum* (3%) (Baruah et al., 2020), coffee husk (4%) (Collazo-Bigliardi et al., 2018), rice straw - banana plant waste (10%) (Ibrahim et al., 2013), and date seeds (17.5%) (Abu-Thabit et al., 2020). In the delignification of Giant reed using 1.25 M NaOH at 90 °C for 5 hours, 34.5% of cellulose was obtained (Tarchoun, et al., 2019a), while on the use of 0.5 M NaOH at 80 °C for 8 hours, 76.89 – 77.67% of cellulose was obtained from para wood dust (Chuayplod and Aht-Ong, 2018). The effectivity of the delignification process can also be reported by the amount of lignin lost, for example as shown by several studies that 42.55% removal of lignin from sago by 10% NaOH at 100 °C for 3 hours (Arnata et al., 2019), and 74.47% removal of lignin from empty palm fruit bunches by 5.5% NaOH at 200 °C for 1 hour (Sebran et al., 2018). These results showed us the effectiveness and flexibility of the alkaline process of delignification from various sources. Therefore, in this study, we applied this method of delignification on the sengon wood sawdust (SWS).

Research has been done on ultrasonic alkali delignification of SWS using 0.5 M NaOH at 40 °C for 30 minutes and reported to yield 77.96% of cellulose (Trisant et al., 2020). However, ultrasonication has a very limited capacity thus not suitable for mass processing like producing pharmaceutical excipients at an industrial scale. We need to find an alternative method that can be run in a scaled-up setup, but many factors such as temperature, time, NaOH concentration, and the ratio of the solvent used are involved. Thus, in this study, we search for the optimal conditions for the delignification of SWS with a more applicable setup by using factorial design analysis. We aim to determine the optimal concentration of NaOH solution and solvent ratio in the delignification process of SWS.

2. EXPERIMENTAL SECTION

2.1 Materials

Sengon wood sawdust (SWS) was obtained as a by-product from CV. Cahaya Abadi Chipp (Kaliwungu-Kendal), from the sandpaper of sengon wood pith processed with machine grid number 250. Sodium hydroxide (NaOH), sodium hypochlorite (NaOCl), and distilled water were used for the delignification.

2.2 Methods

2.2.1 Optimization Variables

Optimization variables are the variables used to determine the optimal condition for SWS cellulose delignification. Variables of NaOH concentration (2% and 10%), temperature (30 °C and 95 °C), reaction time (30 and 360 minutes), and ratio (SWS : NaOH solution) (1:10 and 1:80) were registered for selection with cellulose production as the parameter. From each variable, delignification was done on the lowest and highest values and statistical comparison was applied. Finally, only the parameter with significant differences in the comparison was selected for the determination.

2.2.2 Delignification

Sengon sawdust was dried for 24 hours and then delignified with an optimization design as shown in Table 2. The yields from the delignification treatment were filtered and rinsed until the pH 7.0 and then bleached with 5% NaOCl at 70 °C for 1 hour. The fiber was rinsed with neutral pH waste, dried at 60 °C for 24 hours, and mashed. The final yield obtained is called sengon wood sawdust cellulose (SWSC).

2.2.3 Determination of the Percentages of Cellulose, Hemicellulose, and Lignin

The percentage of cellulose, hemicellulose, and lignin contents in the SWS was determined using the Chesson-Data method (Chesson, 1981).

2.2.4 Optimization Analysis

Each delignification optimization parameter was analyzed using Design Expert software version 10.0.1 where determination was executed based on the highest value of the specified parameters. Comparative tests for the accuracy of the optimization equation of each parameter were carried out using the SPSS 23 program between the predictive data output from Design Expert 10.0.1 and the experimental data.

2.2.5 Characterization of SWSC

Identification, Basic Characterizations, and Purity

The confirmation for cellulose content was done by a blue-violet color formation after the addition of 2 mL of iodized zinc chloride solution to 10 mg of the sample in a test tube. The acidity of the solution was assessed by adding a total of 5 grams of sample to 40 mL of distilled water, stirring for 20 minutes, and measuring the pH with a pH meter (Pachuaui et al., 2019). The confirmation for the purity of cellulose microcrystals was conducted by adding a total of 10 mg of sample to 90 mL of distilled water, followed by heating for 5 minutes, shaking, filtering, and then cooling. The filtrate obtained was then added with 0.1 mL of a 0.05 M iodine solution, and confirmed to be pure when no blue color was formed. Organic impurities were checked by the observation of color change formed from the reaction with 0.5 mL of 0.02 g/mL of phloroglucinol in hydrochloric acid with 10 mg of cellulose. Ash content was checked heating process of 2 g of the sample at 400 °C for 30

minutes followed by 850 °C for 60 minutes (Mukherjee et al., 2018).

Solubility and Loss on Drying

The solubility of the samples was checked on water, H₂SO₄, and NaOH. One gram of samples were dissolved in distilled water until saturated and then filtered using filter paper. The filter paper and the residue were dried in an oven for 3 hours at 105 °C then weighed, cooled in a desiccator, and the final weight was measured for subtraction. For the loss on drying, 1 g of the sample was placed in a porcelain crucible and then dried in an oven at 105 °C for 3 hours or until the weight was constant after two or more measurements (Kharismi and Suryadi, 2018).

Microbial Limit

The microbial limit was carried out using the Total Plate Number method. Five tubes were filled with 9 mL of Peptone Dilution Fluid (PDF) where the sample solutions were diluted with PDF to obtain a yield of 10⁻¹ to 10⁻⁶. Each dilution was pipetted for 1 mL to be put into a Duplo petri dish containing 15 mL of Plate Count Agar (PCA) media at 37±1 °C for 24 hours (yeast) and on Potato Dextrose Agar (PDA) media 25±1 °C for 5x24 hours (fungi).

Particles Morphology and Structure

The cellulose from SWS obtained from the optimum conditions was characterized for the morphology. IR spectra and particle size distribution were compared to Avicel® PH102. The size and the distribution of the cellulose particle from SWS were determined using a Particle Size Analyzer (PSA) (Mastersizer 3000 Malvern Instruments). Scanning Electron Microscopy (SEM) was used to visualize the cellulose surface morphology of SWS (Tarchoun et al., 2019). The SWSC microfibrils were identified by 15 KV acceleration SEM (JEOL JSM-6510LA). Fourier Transform Infrared Spectroscopy (FT-IR) was carried out using an infrared spectrometer (Agilent Technologies Cary 630 FT-IR) with spectra measurements produced in the range of wave numbers 1250-3750 cm⁻¹ (Kian et al., 2017).

3. RESULTS AND DISCUSSION

3.1 Optimization Variables

The selection was done by analyzing if the cellulose productions were significantly different between the processes applying the lowest and the highest value. As shown in Table 1, only the concentration of NaOH and the ratio between SWS and NaOH showed significantly different comparisons between values ($p < 0.05$) and therefore selected for the next optimization step of cellulose delignification. Delignification of cellulose can be influenced by several treatment factors including physical treatment (temperature, time, pressure, and fiber particle size), chemical treatment (acid or base), or a combination of the two as in rice straw (Mukherjee et al., 2018), rice husk (Novia et al., 2019) and biological treatment with the help of microorganisms as in kapuk cortex cellulose isolation (Mi'rajunnisa et al., 2023). Some of the chemical factors that influence the results of delignification are the type, concentration, and ratio

Table 1. Screening of Optimization Variable

Variable		Cellulose (%)	p-value
Concentration of NaOH (%)	2	43.38 ± 0.78	0.005*
	10	54.12 ± 1.63	
Temperature (°C)	30	58.24 ± 0.36	0.088
	95	59.00 ± 0.11	
Time (minute)	30	59.00 ± 0.11	0.069
	360	60.55 ± 0.18	
Ratio (SWS:NaOH solution)	1:10	54.16 ± 1.60	0.000*
	1:80	64.24 ± 0.38	

Note: * ($P < 0.05$ means significantly different)

of fiber weight to the amount of solvent used (Sebran et al., 2018). The optimization variable screening carried out aims to determine a more effective delignification treatment to be further determined as an optimization factor. The results of the screening showed that the NaOH concentration and ratio had a significant effect on the resulting cellulose content (Table 1). This is because NaOH forms a strong alkali which releases heat when dissolved in water and reacts exothermically. NaOH functions as a reducing agent that degrades lignin in lignocellulosic, so it is more effective in breaking lignin and cellulose bonds compared to the effects of physical treatment (temperature and time). Chemical delignification using acid (H₂SO₄ 1%) on wood plants, was more effective as evidenced by an increase in cellulose content of up to 23.9% and a decrease in lignin of 35.1%. Whereas in the physical delignification treatment, the increase in cellulose was only 1.7% with a decrease in lignin of 29.3%. This is because the increase in temperature and time which is very high in the physical delignification treatment does not only break the lignocellulosic bonds but can also damage the structure of the cellulose molecule (Reddy et al., 2013) resulting in a decrease in the degree of crystallinity of cellulose sago fronds (Armata et al., 2019).

3.2 Effect of NaOH Concentration and Ratio (SWS : NaOH Solution) on the Percentage of Hemicellulose, Cellulose, and Lignin

The contents of hemicellulose, cellulose, and lignin produced from the process applying the variations of NaOH concentration and SWS : NaOH ratio are presented in Table 2. Analysis using Design Expert 10 provided Equations 1-3 where the positive value of the coefficient indicates a synergistic and the negative value indicates an antagonistic influence (Karim et al., 2014). From the equations, we found that NaOH concentration (X₁), NaOH ratio (X₂), and the interaction between the two (X₁X₂), have a significant effect ($P < 0.05$) on the hemicellulose (Y₁), cellulose (Y₂), and lignin (Y₃) contents. The analysis

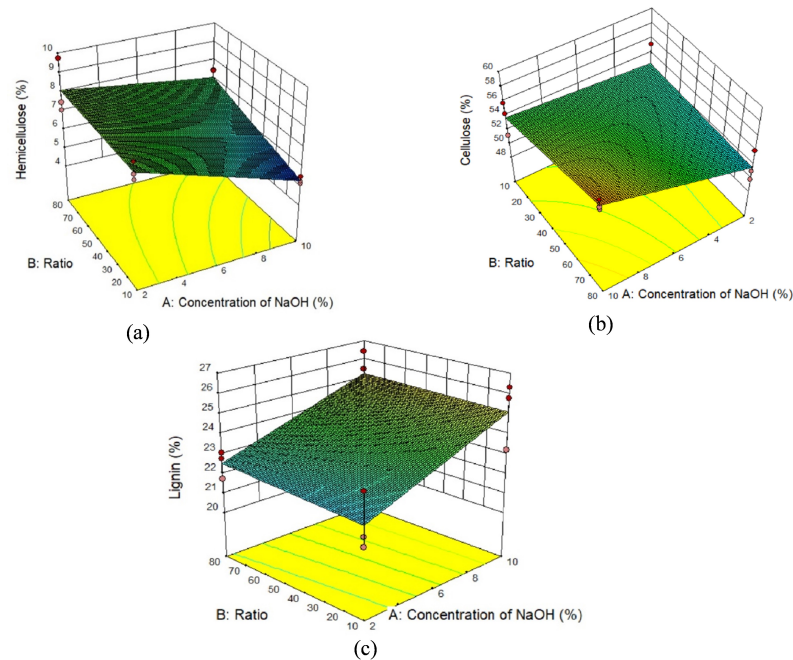


Figure 1. Contour Plot 3D Effect Concentration of NaOH and Ratio (SWS : NaOH Solution) on (a) Hemicellulose; (b) Cellulose; and (c) Lignin

shows that either X_1 or X_2 was reducing the percentage of hemicellulose. However, the reduction was more influenced by the concentration of NaOH than the ratio where the value of X_1 (-0.36) was higher than X_2 ($-4.06 \cdot 10^{-3}$) (Equation 1; Figure 1a). The NaOH concentration increased the cellulose produced from the delignification process of SWS, while the ratio (raw : NaOH solution) did the opposite, as marked by the value of X_1 of $+0.07$ and X_2 of -0.03 (Equation 2; Figure 1b). The effectivity of delignification from SWS can be assessed from the value of the lignin percentage. The process was expected to remove lignin as much as possible, marked by the lowest possible lignin content in the resulting yield. Finally, based on Equation 3, the interaction of two variables X_1X_2 ($-4.76 \cdot 10^{-4}$) would reduce lignin level where the decrease would be more influenced by the ratio than the concentration of NaOH as shown in Figure 1c.

$$Y_1 = 8.70 - 0.36(X_1) - 4.06 \times 10^{-3}(X_2) + 2.86 \times 10^{-3}(X_1X_2) \quad (1)$$

$$Y_2 = 52.61 + 0.07(X_1) - 0.03(X_2) + 8.01 \times 10^{-3}(X_1X_2) \quad (2)$$

$$Y_3 = 21.34 + 0.37(X_1) + 6.57 \times 10^{-3}(X_2) - 4.76 \times 10^{-4}(X_1X_2) \quad (3)$$

Where; Y_1 = Hemicellulose response; Y_2 = Cellulose response; Y_3 = Lignin response; X_1 = Concentration of NaOH; X_2 = Ratio (SWS:NaOH solution).

Variation of NaOH concentration and solvent ratio gave significantly different results on hemicellulose, cellulose, and lignin concentrations. Equations 1-3 show that an increase in the concentration of NaOH (X_1) has a synergistic (positive) relationship with the cellulose content. This is because the higher the concentration of NaOH used, the reaction will occur causing many broken aryl-ester, carbon-carbon, and alkyl-alkyl bonds. So that the lignocellulosic bond will be released which is marked by the formation of a blackish brown solution. NaOH as a strong alkali is not only able to break lignocellulosic bonds but will also change monosaccharides and end groups on polysaccharides (1,4 glycosidic and hemicellulose bonds) into various carboxylic acids by breaking bonds from end to end. Part of the cellulose chain that is left over from this process is a compound called α -cellulose. Hemicellulose is more sensitive to bases when compared to lignin and cellulose (Reddy et al., 2013), this causes an antagonistic (negative) relationship to be seen from increasing the concentration of NaOH (X_1) with hemicellulose levels.

The hemicellulose (Y_1) and cellulose (Y_2) equations show that the hemicellulose and cellulose levels have an antagonistic (negative) relationship with the SWS and solvent ratio variables, where the greater the ratio the lower the hemicellulose content. Hemicellulose is easily soluble in water (hydrophilic), easily expands, and has short and branched bonds so that the

Table 2. Design and Optimization Response to Delignification of Cellulose from SWS

Run	Concentration of NaOH (%)	Ratio (SWS : NaOH solution)	Time (min)	Temperature (°C)	Hemicellulose (%)	Cellulose (%)	Lignin (%)
1	2	1:80	30	50	7.08	49.86	23.09
2	2	1:80	30	50	7.49	54.05	21.75
3	2	1:80	30	50	9.75	51.06	22.79
4	10	1:10	30	50	5.52	51.26	26.32
5	10	1:10	30	50	5.17	55.82	23.23
6	10	1:10	30	50	5.29	54.38	25.78
7	10	1:80	30	50	6.25	56.78	25.47
8	10	1:80	30	50	7.47	58.16	26.44
9	10	1:80	30	50	7.42	57.10	23.80
10	2	1:10	30	50	8.47	55.31	21.62
11	2	1:10	30	50	7.62	50.33	21.14
12	2	1:10	30	50	7.88	52.21	23.69

solvent penetrates more easily into it (Abraham et al., 2011). This causes the breaking of polysaccharide bonds so that hemicellulose is more easily dissolved. While cellulose is composed of units β -D-glucopyranose with glycosidic linkages (1-4). Cellulose molecules are linear and have hydrogen bonds so their solubility is low, but the -OH group on cellulose causes the surface to become hydrophilic (Siqueira et al., 2010). So with an increase in the ratio, the interaction of cellulose and water molecules will be easier and the cellulose content will decrease. The interaction between the two variables, namely NaOH content, and ratio, showed a synergistic (positive) effect on hemicellulose and cellulose levels. However, the coefficient of increase in cellulose is greater ($+8.01 \times 10^{-3}$) than hemicellulose ($+2.86 \times 10^{-3}$), this indicates that the interaction effect of cellulose and water molecules is lower than the ability of NaOH to delignification cellulose.

The synergistic effect is seen in the effect of NaOH levels (X_1) and the ratio (X_2) on lignin content. Lignin is a three-dimensional polymer compound consisting of phenol propane units with C-O-C and C-C bonds. The arylakil bond (C-C) of the ester bond makes lignin resistant to hydrolysis. Lignin is insoluble in water and difficult to degrade because of its complex and heterogeneous structure. The same results were seen in the delignification of kenaf fiber as evidenced by FTIR analysis showing the loss of C=O at the absorption peak that previously appeared before treatment, but there was an appearance at another absorption peak indicating that lignin was not completely reduced after NaOH treatment. The presence of absorption peaks of O-H groups (stretching) which is a component of cellulose bound to lignin indicates that lignin has not been completely reduced and needs further treatment. Such as In the delignification of Stipa Obtusa fibers which showed that most of the lignin and hemicellulose remaining after the alkaline treatment was removed during bleaching (Chavez et al., 2023). However, at the right concentration and solvent ratio, delignification treatment with NaOH can reduce lignin con-

centrations. It can be seen that there is an antagonistic effect on the X_1X_2 interaction (-4.76×10^{-4}) because the OH- ions from NaOH can react with the phenolic ring in lignin so that it can increase its hydrophilicity. Delignification of NaOH can remove up to 54% of lignin in palm kernel cellulose (Hii and Mashitah, 2014) and 62.7% in empty palm fruit bunches (Zawawi et al., 2018).

3.3 Optimization of Cellulose Delignification From SWS

Optimum conditions for cellulose delignification from SWS were obtained based on a regression model of the desirability of hemicellulose, cellulose, and lignin content. These conditions were optimized to degrade hemicellulose and lignin to obtain maximized cellulose content in the selected ranges that have been determined for the priority from high to low for each of cellulose, lignin, and hemicellulose at the weight of 0.1-1. Furthermore, the optimization analysis would provide a desirability function, which in this study, each expected response value is considered individually as an objective function and the desirability function is developed to obtain optimal conditions (Mesa et al., 2017). As results from the model analysis, the optimum conditions for cellulose delignification from SWS was using 2% NaOH solution with a ratio of 1 : 19.20, with the predicted percentage of 8.01% for hemicellulose, 52.49% for cellulose, and 22.20% for lignin. These conditions result in the desirability of 0.849. This high desirability value (from the maximum of 1) indicates that the system would produce predicted results close to the ideal (Amdoun et al., 2018). To confirm this finding, a t-test comparison analysis was conducted between the predicted data and the experimental results of the concentrations of hemicellulose, cellulose, and lignin. It was shown that the levels of hemicellulose, cellulose, and lignin between the predicted and experimental data were not significantly different ($P > 0.05$) as shown in Table 3.

Table 3. Comparative Analysis of Predictions and Observed Data

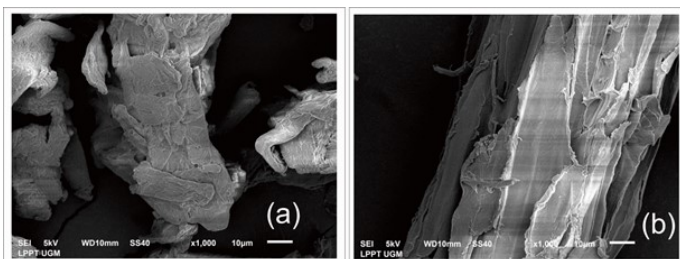
The response	Prediction	Research \pm SD	<i>p</i> -value
Hemicellulose (%)	8.01	7.86 \pm 0.28	0.310
Cellulose (%)	52.49	52.47 \pm 0.77	0.956
Lignin (%)	22.20	21.62 \pm 0.85	0.202

Note: ($P < 0.05$ means significantly different)

3.4 Cellulose Characterization of SWS

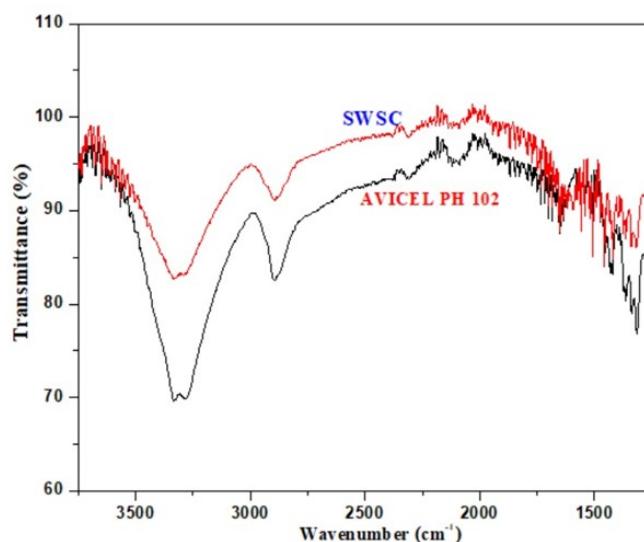
The SWSC obtained from the delignification process was an off-white, tasteless, and odorless fine powder. The results of the cellulose characterization of SWS are presented in Table 4. The presence of cellulose was identified with the formation of a violet-blue color as also found in SWSC. Starch was not identified in the resulting SWSC. Organic impurities found in the SWS were no longer found after the delignification process, confirmed by the negative result in the SWSC. The other confirmed characteristics are according to the following pharmaceutical standards pH of 5-7, ash content of $\leq 0.1\%$, loss on drying of less than 7%, the microbial limit of 10^3 cfu/g, slightly soluble in 5% NaOH, and practically insoluble in water and HCl (Sheskey et al., 2017).

The test results show that SWSC has characteristics that comply with pharmaceutical excipient standards with a neutral pH value which is expected to be inert and not incompatible with active ingredients. This indicates that the prepared cellulose is simply washed with water after extraction. There is a SWSC mineral content at standard limits which are expected not to affect the quality of the resulting preparations. The solubility of SWSC in slightly soluble NaOH indicates the presence of long-chain cellulose and is the highest purity level of cellulose which is often referred to as α -cellulose (Trache et al., 2016). Loss on drying SWSC (7%) was lower than SWS (8.62%), this indicated that the delignification process was able to reduce the number of compounds lost in the drying process.

**Figure 2.** SEM Images of (a) Avicel® PH 102 and (b) SWSC

All of this characterization information is important to know as a basis for considering the use of cellulose, especially in the pharmaceutical industry. Several tests were carried out by the cellulose test in the handbook of pharmaceutical excipients, which is a quality standard for pharmaceutical excipients such as identification, starch, organic impurities, loss on drying

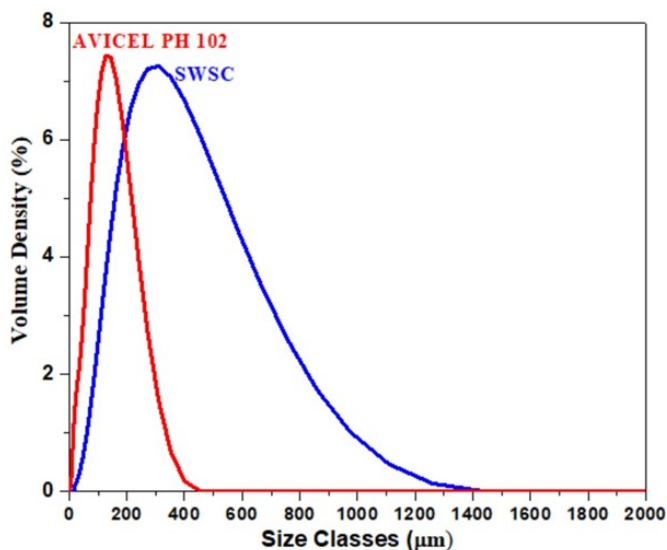
cellulose and ash content, to ensure the purity of the SWSC produced so that it is expected that there are no other impurities when used in the formulation pharmaceutical preparations including microbial contamination as evidenced by microbial limit tests with the result below the standard limit. Pharmaceutical dosage forms vary in solid, semi-solid, and liquid so SWSC solubility information will be very necessary when selecting excipients according to the target dosage form to be made.

**Figure 3.** FT-IR Spectrum of Avicel® PH 102 and SWSC

In addition to the characterization test to confirm the constituent groups of cellulose, FTIR analysis was also carried out. The typical chemical bonds to check to identify cellulose structure in this study are C-O (stretching) at $(1300-1000)$ cm^{-1} , -OH (stretching) at $(3650-3200)$ cm^{-1} , and CH (stretching) at $(3000-2850)$ cm^{-1} . The FT-IR spectra of SCWS and commercial cellulose (Avicel® PH 102) can be seen in Figure 3. Both spectra show identical patterns with the -OH functional group detected at 3400 cm^{-1} as in-plane deformation and the C-O stretching vibration group with peaks at 1025 cm^{-1} . The presence of the C-H group with stretching and bending vibrations is shown at 2875 cm^{-1} . 1,4- β -glycosidic produces -CH vibrations which indicate the presence of cellulose from the appearance of a signal at around 2875 cm^{-1} . The presence of acetyl groups and hemicellulose ester groups or carboxyl groups in lignin are shown in the spectra that appear in the 1700 cm^{-1} area which is marked with the C=O. There is no peak at 1700 cm^{-1} which indicates that by delignification treatment, the non-cellulose content in SWSC was lost because it is dissolved in the solvent used. In addition, the C=C (stretching) of the aromatic chain in lignin is absent the the spectra indicating the partial elimination of lignin and hemicellulose (Abdul Rahman et al., 2017). The spectra formed at 1009 cm^{-1} – 1147 cm^{-1} are C-O-C (stretching) vibrations of hemicellulose and cellulose components (Pujiasih et al., 2018).

Table 4. Characteristics of SWSC

Characteristics	SWS	SWSC
Identification	Violet-blue	Violet-blue
pH	7.0	7.0
Starch	Nil	Nil
Organic impurities	Positif	Nil
Hemicellulose (%)	9.14	7.86
Cellulose (%)	50.85	52.47
Lignin (%)	24.37	21.62
Ash (%)	0.44	0.92
Solubilty	Practically insoluble in water, 5% NaOH and HCl	Slightly soluble in 5% NaOH, practically insoluble in water and HCl
Loss on drying (%)	8.62	7.00
Microbial limit		
The total plate number (cfu/g)	1,9 x 10 ²	0
The yeast fungus number (cfu/g)	3,3 x 10 ²	2,0 x 10 ²

**Figure 4.** Particle Size Distribution Profiles of SWSC and Avicel® PH 102

The spectra generated from the SWSC analysis confirmed that cellulose was proven by the SWSC spectra to have the same pattern as commercial cellulose (Avicel® PH 102). In these results, it was found that there was a spectrum of cellulose while the absorption band characteristics of lignin and hemicellulose were not found this indicates that the non-cellulose component has been removed in the delignification process. Sesame hull cellulose pretreatment results also showed the same result (Zhang et al., 2021).

The particle size average of SWSC was larger than the commercial cellulose Avicel® PH 102, with homogeneous distribution as shown in Figure 4. The results of measuring SWSC and Avicel® PH 102 particles at Dx (10) were 106,783

µm and 26.57 µm respectively; Dx (50) were 289,493 µm and 110,489 µm; Dx (90) were 654.724 µm and 234.472 µm; and Dx (100) were 1428,986 µm and 452,794 µm. SEM images in Figure 2 show that the morphology of SWSC (Figure 2b) and commercial cellulose (Avicel® PH 102) (Figure 2a) looks similar in the form of plates. The cross-sectional images show a porous and dense layer, with a wide range of pore sizes.

Particle size distribution and the results of the SWSC SEM analysis greatly determine its ability as a solid dosage excipient because uniform particle shape and size can determine the flow properties of the powder which affects the compressibility and uniformity of the resulting tablet weights, especially for direct compress. by damage to the pore walls due to the merging of several small pore walls to become larger. The two SEM results show that the non-uniform size can be caused by the very wide range of cellulose molecular weights. The results are similar to the morphology of rosella cellulose fibers (Kian et al., 2017), and grapefruit peel (Liu et al., 2018). The rod-shaped SWSC structure looks like a sheet with a compact structure (Figure 2b), as can be seen in the cellulose structure of maize straw (Yu et al., 2020). These results indicate the presence of free cellulose in which lignin and hemicellulose have been removed in the delignification process.

4. CONCLUSION

NaOH concentration and ratio (SWS: NaOH solution) on the cellulose delignification from sengon wood sawdust had a significant effect on the concentration of hemicellulose, cellulose, and lignin ($P < 0.05$). Optimum conditions with the factorial design method of cellulose delignification process from sengon wood sawdust used a 2% NaOH solution ratio (1:19.20) at the predicted concentrations of hemicellulose 8.01%, cellulose 52.49%, and lignin 22.2%. One sample T-test analysis of predictive and research values of hemicellulose, cellulose, and lignin showed insignificant results ($P > 0.05$) which means that

the optimization equation proved valid to determine the optimum conditions for cellulose delignification of sengon wood sawdust. The cellulose produced under these conditions has similar characteristics according to the standard with FT-IR and SEM to Avicel® PH 102.

5. ACKNOWLEDGMENT

The author would like to express his gratitude for The Indonesian Education Scholarship Program (BPI) within the Indonesian Ministry of Education and Culture (Kemendikbud RI) funded by the Indonesian Endowment Fund for Education (LPDP).

REFERENCES

- Abdul Rahman, N. H., B. W. Chieng, N. A. Ibrahim, and N. Abdul Rahman (2017). Extraction and Characterization of Cellulose Nanocrystals from Tea Leaf Waste Fibers. *Polymers*, **9**(11); 588
- Abraham, E., B. Deepa, L. A. Pothan, M. Jacob, S. Thomas, U. Cvelbar, and R. Anandjiwala (2011). Extraction of Nanocellulose Fibrils from Lignocellulosic Fibres: A Novel Approach. *Carbohydrate Polymers*, **86**(4); 1468–1475
- Abu-Thabit, N. Y., A. A. Judeh, A. S. Hakeem, A. Ul-Hamid, Y. Umar, and A. Ahmad (2020). Isolation and Characterization of Microcrystalline Cellulose from Date Seeds (*Phoenix dactylifera* L.). *International Journal of Biological Macromolecules*, **155**; 730–739
- Amdoun, R., L. Khelifi, M. Khelifi-Slaoui, S. Amroune, M. Asch, C. Assaf-Ducrocq, and E. Gontier (2018). The Desirability Optimization Methodology; A Tool to Predict Two Antagonist Responses in Biotechnological Systems: Case of Biomass Growth and Hyoscyamine Content in Elicited *Datura starmonium* Hairy Roots. *Iranian Journal of Biotechnology*, **16**(1); 11–19
- Ameram, N., S. Muhammad, N. A. A. N. Yusof, S. Ishak, A. Ali, N. F. Shoparwe, and T. P. Ter (2019). Chemical Composition in Sugarcane Bagasse: Delignification with Sodium Hydroxide. *Malaysian Journal of Fundamental and Applied Sciences*, **15**(2); 232–236
- Arnata, I. W., F. Fahma, N. Richana, and T. C. Sunarti (2019). Cellulose Production from Sago Frond with Alkaline Delignification and Bleaching on Various Types of Bleach Agents. *Oriental Journal of Chemistry*, **35**(1); 8–19
- Bangar, S. P., O. J. Esua, C. Nickhil, and W. S. Whiteside (2023). Microcrystalline Cellulose for Active Food Packaging Applications: A Review. *Food Packaging and Shelf Life*, **36**; 101048
- Baruah, J., R. C. Deka, and E. Kalita (2020). Greener Production of Microcrystalline Cellulose (MCC) from *Saccharum spontaneum* (Kans grass): Statistical Optimization. *International Journal of Biological Macromolecules*, **154**; 672–682
- Chavez, B. K., G.-P. Karen, D. C. Parada, and E. Flores (2023). Thermochemical Isolation and Characterization of Nanofibrillated Cellulose from *Stipa obtusa* Fibers. *Carbohydrate Polymer Technologies and Applications*, **6**; 100344
- Cheng, F., X. Zhao, and Y. Hu (2018). Lignocellulosic Biomass Delignification using Aqueous Alcohol Solutions with the Catalysis of Acidic Ionic Liquids: A Comparison Study of Solvents. *Bioresource Technology*, **249**; 969–975
- Chesson, A. (1981). Effects of Sodium Hydroxide on Cereal Straws in Relation to the Enhanced Degradation of Structural Polysaccharides by Rumen Microorganisms. *Journal of the Science of Food and Agriculture*, **32**(8); 745–758
- Chuayplod, P. and D. Aht-Ong (2018). A Study of Microcrystalline Cellulose Prepared from Parawood (*Hevea brasiliensis*) Sawdust Waste using Different Acid Types. *Journal of Metals, Materials and Minerals*, **28**(2); 106–114
- Collazo-Bigliardi, S., R. Ortega-Toro, and A. C. Boix (2018). Isolation and Characterisation of Microcrystalline Cellulose and Cellulose Nanocrystals from Coffee Husk and Comparative Study with Rice Husk. *Carbohydrate Polymers*, **191**; 205–215
- Hartati, N. S., E. Sudarmonowati, W. Fatriasari, E. Hermiati, W. Dwianto, R. Kaida, K. Baba, and T. Hayashi (2010). Wood Characteristic of Superior Sengon Collection and Prospect of Wood Properties Improvement through Genetic Engineering. *Wood Research Journal*, **1**(2); 103–107
- Hii, K. L. and M. D. Mashitah (2014). Optimisation of Pressed Pericarp Fibre Delignification for Glucose Recovery using Response Surface Methodology. *International Journal of Environmental Engineering*, **6**(2); 220–238
- Ibrahim, M. M., W. K. El-Zawawy, Y. Jüttke, A. Koschella, and T. Heinze (2013). Cellulose and Microcrystalline Cellulose from Rice Straw and Banana Plant Waste: Preparation and Characterization. *Cellulose*, **20**(5); 2403–2416
- Karim, M. Z., Z. Z. Chowdhury, S. B. Abd Hamid, and M. E. Ali (2014). Statistical Optimization for Acid Hydrolysis of Microcrystalline Cellulose and Its Physiochemical Characterization by Using Metal Ion Catalyst. *Materials*, **7**(10); 6982–6999
- Kharismi, R. R. A. Y. and H. Suryadi (2018). Preparation and Characterization of Microcrystalline Cellulose Produced from Betung Bamboo (*Dendrocalamus asper*) through Acid Hydrolysis. *Journal of Young Pharmacists*, **10**(2); 79–83
- Kian, L. K., M. Jawaid, H. Ariffin, and O. Y. Alothman (2017). Isolation and Characterization of Microcrystalline Cellulose from Roselle Fibers. *International Journal of Biological Macromolecules*, **103**; 931–940
- Krivokapić, J., J. Ivanović, J. Djuriš, D. Medarević, Z. Potpara, Z. Maksimović, and S. Ibrić (2020). Tableting Properties of Microcrystalline Cellulose Obtained from Wheat Straw Measured with a Single Punch Bench Top Tablet Press. *Saudi Pharmaceutical Journal*, **28**(6); 710–718
- Kundu, C., S. P. Samudrala, M. A. Kibria, and S. Bhattacharya (2021). One-Step Peracetic Acid Pretreatment of Hardwood and Softwood Biomass for Platform Chemicals Production. *Scientific Reports*, **11**(1); 11183
- Laksono, A. D., T. F. Susanto, R. Dikman, J. Awali, N. Sasria,

- and I. Y. Wardhani (2022). Mechanical Properties of Particleboards Produced from Wasted Mixed Sengon (*Paraserianthes falcataria* (L.) Nielsen) and Bagasse Particles. *Materials Today: Proceedings*, **65**; 2927–2933
- Liu, Y., A. Liu, S. A. Ibrahim, H. Yang, and W. Huang (2018). Isolation and Characterization of Microcrystalline Cellulose from Pomelo Peel. *International Journal of Biological Macromolecules*, **111**; 717–721
- Mesa, L., Y. Martínez, E. Barrio, and E. González (2017). Desirability Function for Optimization of Dilute Acid Pretreatment of Sugarcane Straw for Ethanol Production and Preliminary Economic Analysis based in Three Fermentation Configurations. *Applied Energy*, **198**; 299–311
- Mirajunnisa, H. Suryadi, Sutriyo, and Y. P. I. Lestari (2023). Isolation of Cellulase from Selected Fungal Strains and its use for Manufacture Microcrystal Cellulose from Kapuk Cortex (*Ceiba pentandra* (L.) Gaertn). *Science and Technology Indonesia*, **8**(2); 227–234
- Mukherjee, A., S. Banerjee, and G. Halder (2018). Parametric Optimization of Delignification of Rice Straw through Central Composite Design Approach Towards Application in Grafting. *Journal of Advanced Research*, **14**; 11–23
- Novia, N., V. K. Pareek, H. Hermansyah, and A. M. Jannah (2019). Effect of Dilute Acid-Alkaline Pretreatment on Rice Husk Composition and Hydrodynamic Modeling with CFD. *Science and Technology Indonesia*, **4**(1); 18–23
- Pachau, L., R. S. Dutta, L. Hauzel, T. B. Devi, and D. Deka (2019). Evaluation of Novel Microcrystalline Cellulose from *Ensete glaucum* (Roxb.) Cheesman Biomass as Sustainable Drug Delivery Biomaterial. *Carbohydrate Polymers*, **206**; 336–343
- Pujiasih, S., A. Masykur, T. Kusumaningsih, and O. A. Saputra (2018). Silylation and Characterization of Microcrystalline Cellulose Isolated from Indonesian Native Oil Palm Empty Fruit Bunch. *Carbohydrate Polymers*, **184**; 74–81
- Rahmawati, D., N. Khumaida, and U. J. Siregar (2019). Morphological and Phytochemical Characterization of Susceptible and Resistant Sengon (*Falcataria moluccana*) Tree to Gall Rust Disease. *Biodiversitas Journal of Biological Diversity*, **20**(3); 907–913
- Reddy, K. O., C. U. Maheswari, M. Shukla, J. Song, and A. V. Rajulu (2013). Tensile and Structural Characterization of Alkali Treated Borassus Fruit Fine Fibers. *Composites Part B: Engineering*, **44**(1); 433–438
- Sanchez, D. R. (2007). Reausticizing: Principles and Practice. *Vector Process Equipment Inc*; 2–1
- Sebran, N. H., L. P. Gaik, and A. S. Hussain (2018). Structural Analysis on the Effect of Base-Catalysed Delignification Process Parameters on Palm Oil Empty Fruit Bunches Fibres using Glycome Profiling. In *IOP Conference Series: Materials Science and Engineering*, volume 458. IOP Publishing, pages 1–8
- Sheskey, P., W. Cook, and C. Cable (2017). *Handbook of Pharmaceutical Excipients*. Pharmaceutical Press
- Siqueira, G., J. Bras, and A. Dufresne (2010). Cellulosic Nanocomposites: A Review of Preparation, Properties and Applications. *Polymers*, **2**(4); 728–765
- Siregar, U. J., D. Rahmawati, and A. Damayanti (2019). Fingerprinting Sengon (*Falcataria moluccana*) Accessions Resistant to Baktor Pest and Gall Rust Disease using Microsatellite Markers. *Biodiversitas Journal of Biological Diversity*, **20**(9); 2698–2706
- Sudarsono, W., W. Y. Wong, K. S. Loh, E. H. Majlan, N. Syarif, K.-Y. Kok, R. M. Yunus, K. L. Lim, and I. Hamada (2020). Sengon Wood-Derived RGO supported Fe-based Electrocatalyst with Stabilized Graphitic N-bond for Oxygen Reduction Reaction in Acidic Medium. *International Journal of Hydrogen Energy*, **45**(43); 23237–23253
- Taher, T., S. Maulana, N. Mawaddah, A. Munandar, A. Rianjanu, and A. Lesbani (2023). Low-Temperature Hydrothermal Carbonization of Activated Carbon Microsphere Derived from Microcrystalline Cellulose as Carbon Dioxide (CO₂) Adsorbent. *Materials Today Sustainability*; 100464
- Tarchoun, A. F., D. Trache, and T. M. Klapötke (2019). Microcrystalline Cellulose from *Posidonia oceanica* Brown Algae: Extraction and Characterization. *International Journal of Biological Macromolecules*, **138**; 837–845
- Trache, D., M. H. Hussin, C. T. H. Chuin, S. Sabar, M. N. Fazita, O. F. Taiwo, T. Hassan, and M. M. Haafiz (2016). Microcrystalline Cellulose: Isolation, Characterization and Bio-Composites Application—A Review. *International Journal of Biological Macromolecules*, **93**; 789–804
- Trisant, P. N., I. Gunardi, and Sumarno (2020). The Influence of Hydrolysis Time in Hydrothermal Process of Cellulose from Sengon Wood Sawdust. In *Macromolecular Symposia*, volume 391. Wiley Online Library, page 2000016
- Wang, J., Z. Liu, Y. Zheng, Q. Hong, Q. Wang, and X. Xu (2023). Synergistic Effects of Microcrystalline Cellulose and Xanthan Gum on the Stability of Milk Fat-Based UHT Whipping Cream. *LWT*, **184**; 114966
- Yu, H., J. Wang, J. Yu, Y. Wang, and R.-a. Chi (2020). Adsorption Performance and Stability of the Modified Straws and their Extracts of Cellulose, Lignin, and Hemicellulose For Pb²⁺:pH Effect. *Arabian Journal of Chemistry*, **13**(12); 9019–9033
- Zawawi, A. Z., L. P. Gaik, N. H. Sebran, J. Othman, and A. S. Hussain (2018). An Optimisation Study on Biomass Delignification Process using Alkaline Wash. *Biomass Conversion and Biorefinery*, **8**(1); 59–68
- Zhang, R.-Y., H.-M. Liu, J. Hou, Y.-G. Yao, Y.-X. Ma, and X.-D. Wang (2021). Cellulose Fibers Extracted from Sesame Hull using Subcritical Water as a Pretreatment. *Arabian Journal of Chemistry*, **14**(6); 103178